Chemical Science

ROYAL SOCIETY OF CHEMISTRY

REVIEW

View Article Online
View Journal | View Issue

Cite this: *Chem. Sci.*, 2022, **13**, 9833

Organic radicals with inversion of SOMO and HOMO energies and potential applications in optoelectronics

Sitthichok Kasemthaveechok, [a] Laura Abella, [b] Jeanne Crassous, [a] Jochen Autschbach *[b] and Ludovic Favereau *[a]

Received 3rd May 2022
Accepted 6th July 2022

DOI: 10.1039/d2sc02480b

rsc.li/chemical-science

Organic radicals possessing an electronic configuration in which the energy of the singly occupied molecular orbital (SOMO) is below the highest doubly occupied molecular orbital (HOMO) level have recently attracted significant interest, both theoretically and experimentally. The peculiar orbital energetics of these SOMO–HOMO inversion (SHI) organic radicals set their electronic properties apart from the more common situation where the SOMO is the highest occupied orbital of the system. This review gives a general perspective on SHI, with key fundamental aspects regarding the electronic and structural factors that govern this particular electronic configuration in organic radicals. Selected examples of reported compounds with SHI are highlighted to establish molecular guidelines for designing this type of radical, and to showcase the potential of SHI radicals in organic spintronics as well as for the development of more stable luminescent radicals for OLED applications.

Introduction

Organic radicals form a particular class of materials exhibiting an open-shell electronic structure with one or more unpaired electrons (Fig. 1). Radical compounds are often considered as highly sensitive, and they usually react quickly *via* dimerization, hydrogen abstraction, or other degradation mechanisms. With the continuous development of organic chemistry and the deeper experimental and theoretical understanding of the parameters controlling molecular reactivity, a number of stable or persistent organic open-shell compounds have been isolated and investigated. As a result of their specific (photo-)reactivity, radicals have continued to attract significant interest in chemistry and biochemistry, notably playing a central role in many enzymatic reactions as well as *in vivo* imaging.[1–3] Organic π-conjugated radicals are also the subject of intense research in materials science because of their electron spin, making them innovative alternatives for the basis of next-generation optoelectronics, for instance, in organic field-effect transistors (OFETs),[4–6] organic light-emitting diodes (OLEDs), or organic magnets.[4,5,7–27] Furthermore, these molecular materials also provide fundamental insights about the nature of chemical bonds and their delocalization in open-shell systems, in addition to their other features such as narrow HOMO–LUMO energy gaps, low-lying doubly-excited states, or redox amphoterism.[4,10,12,13,15,28,29]

In the popular molecular orbital (MO) description of electronic structure, as widely adopted in chemistry and related fields,[30] an unpaired electron means the set of MOs includes

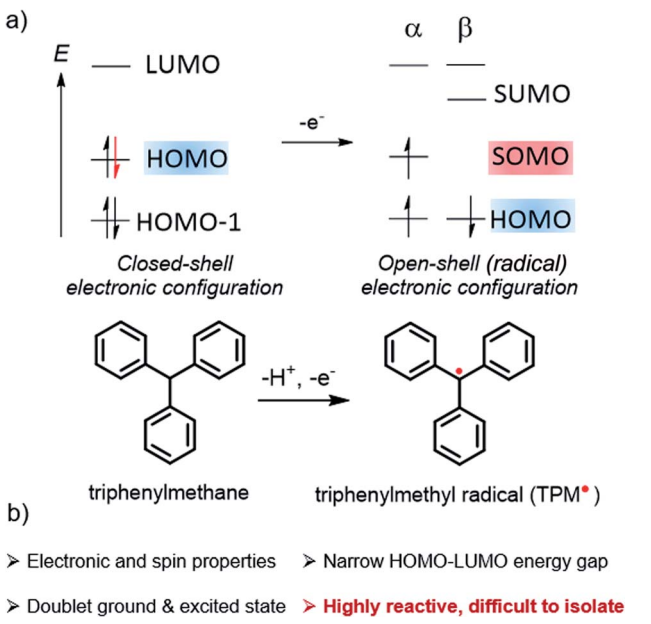

Fig. 1 (a) Schematic comparison of the frontier orbitals of a neutral closed-shell *vs.* an open-shell compound. The latter is obtained from the former by a one electron oxidation process and shows the SOMO as the highest energy level and its unoccupied (SUMO) counterpart, illustrated here with the triphenylmethane and corresponding triphenylmethyl radical, TPM•. (b) Key optoelectronic properties of an organic radical.

[a]*Univ Rennes, CNRS, ISCR – UMR 6226, F-35000 Rennes, France. E-mail: ludovic.favereau@univ-rennes1.fr*

[b]*Department of Chemistry, University at Buffalo, State University of New York, Buffalo, New York 14260, USA. E-mail: jochena@buffalo.edu*

a singly occupied molecular orbital (SOMO, Fig. 1), that is, an occupied α spin ('spin-up' ↑) or β spin ('spin-down' ↓) orbital without a matching occupied opposite-spin (β or α) counterpart with the same or very similar spatial behaviour (spatial function). The spatial function is what defines the two-colored isosurface plots seen in research articles and textbooks for depictions of MOs; the SOMO spatial function and the unpaired spin are of course intimately connected to the radical properties.

For the radical in Fig. 1, the α and β spin components of the HOMO are assumed to have matching spatial functions, and are therefore grouped as a spin pair. Likewise, the SOMO and its unoccupied spin counterpart, which we label SUMO for convenience, are assumed to have matching spatial functions, but only one of them is occupied. As drawn, the figure reflects the fact that in spin-unrestricted MO self-consistent field (SCF) calculations, the α and β spin orbitals may have different energies, even if their spatial functions match closely. This is the case, in particular, for the SOMO–SUMO pair.

Since the pioneering works of Thiele and Chichibabin on open-shell hydrocarbons,[31–33] significant efforts have been directed toward understanding the structural and electronic factors that may lead to an increased stability of radical systems. When discussing this crucial aspect, it is important to differentiate between the terms stable and persistent for quantifying the reactivity of a radical by using the advice of Ingold, who wrote that[34] "[…] the word stable should only be used to describe a radical so persistent and so unreactive to air, moisture, *etc.*, under ambient conditions that the pure radical can be handled and stored in the lab with no more precautions than would be used for the majority of commercially available organic chemicals". Thus, most long-lived radicals deserve to be labeled persistent, and few rise to the level of stable.

The challenge for chemists is to design organic radicals that are as persistent as possible, to investigate their specific properties in depth, and to take advantage of these properties in optoelectronic and other types of applications. To reach this objective, an old and rather simple approach is to introduce bulky substituents to prevent dimerization or reaction with molecular oxygen, for instance. This strategy is often quite efficient to increase the kinetic stability of a radical compound. Another approach involves the delocalization of the unpaired electron along a molecular backbone, which reduces the accumulation of spin density at certain atoms and tends to increase the overall radical stability. Very recently, Paton *et al.* proposed a quantitative description of the term stability for radicals based on a combination of thermodynamic and kinetic factors,[35] which can be related to the aforementioned delocalization and steric protection approaches, respectively.

In addition to gaining fundamental insight regarding the reactivity of organic radicals, investigations of these species have also furnished a better understanding of how the presence of unpaired electrons influences the optical, electronic and magnetic properties of a molecule. For instance, the ground state of a mono-radical and its lowest excited state, accessible *via* spin-allowed processes, are of spin-doublet nature,[36,37] which can offer new opportunities for optoelectronic

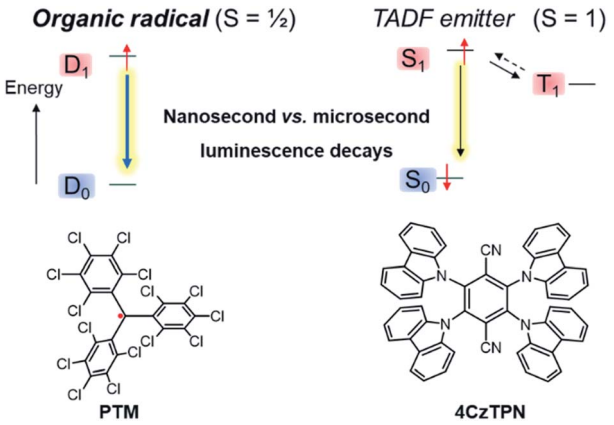

Fig. 2 Comparison of the emission process of the organic radical emitter *per*-chlorotriphenylmethyl **PTM** (left) and the TADF emitter 2,3,5,6-tetra(9*H*-carbazol-9-yl)terephthalonitrile, **4CzTPN** (right).[44]

applications and especially in OLED technology.[14,16,17,38–41] Considered as a curiosity for a long time, this type of luminescence is currently attracting strong interest because doublet radicals do not give rise to dark triplet states, unlike classical fluorescent organic emitters with closed-shell electronic configuration (Fig. 2). Accordingly, radicals offer the potential to reach a theoretical internal quantum efficiency (IQE) of 100% in OLEDs, whereas the IQE is *ca.* 25% for classical fluorophore compounds. Furthermore, the nanosecond luminescence lifetime of radicals is highly beneficial for display applications, in comparison to the microseconds found for thermally activated delayed fluorescence (TADF) materials.[37,42] In the latter process, the reverse intersystem crossing rate, illustrated by the dashed arrow from T_1 to S_1 in Fig. 2, is low and often competes with non-radiative quenching, causing poor device efficiency at high brightness levels.[43]

Beyond mono-radicals, the design of organic molecules containing at least two interacting unpaired electrons, such as diradicals, is of particular interest, because of the multiplicity of the spin states and their energetic ordering, which is related to the strength of the interaction between the unpaired electrons.[7,45,46] For example, in the case of a di-radical the stability of

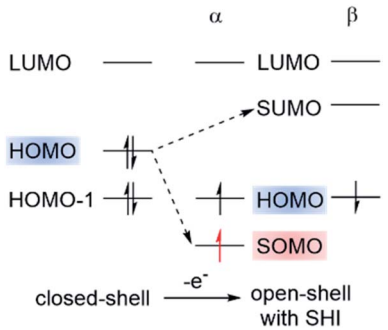

Fig. 3 Schematic representation of the electronic configuration found in organic radicals with SOMO–HOMO inversion (SHI). Figure adapted with permission from ref. 53. Copyright 2021 American Chemical Society.

the triplet *vs.* an open-shell singlet spin state becomes important. Different accessible spin states provide a molecular system with switchable magnetic properties, and the possibility of a high-spin ground state,[45–47] which is desirable for molecular-scale spin information processing and memory devices. Polymeric radicals have also been investigated, with recent examples displaying high conductivity properties[48] as well as high spin multiplicity.[49]

One typical feature of an organic mono-radical is that the SOMO has higher energy than the doubly occupied MOs in the ground-state electronic configuration (Fig. 1). This is associated with the *aufbau* rule, by which orbitals are occupied by up to two electrons (counting a pair of α and β orbitals with matching (identical or very similar) spatial functions as a single orbital in this context) from low to high orbital energy. This concept is extremely useful in chemistry for rationalizing the electronic structure and reactivity of molecules. However, it is important to note that a change in the electronic configuration, for example from ionisation or electron reduction of a molecule, or an excitation, impacts all orbitals of the system. In other words, the spatial functions (orbital shapes) as well as the orbital energies change in response to a change in the electron configuration. This means the 'ladder of MOs' of a system is not rigid.[30,50,51] For example, changes in the inter-orbital repulsion must be considered when assessing the relative stability of different alternative electron configurations. A case in point is the 3d–4s inversion of filling order for neutral first-transition row atoms: the partially filled 3d shell in the atomic ground states is energetically below the singly or doubly occupied 4s,[52] in apparent violation of the *aufbau* rule.

Recently, a violation of the *aufbau* rule has also been claimed for certain organic radicals. These systems possess an electronic configuration in which the energy of the SOMO is below the HOMO level (Fig. 3). This SOMO–HOMO inversion (SHI), alternatively referred to as SOMO–HOMO conversion or a quasi-closed-shell configuration, has generated widespread interest, both theoretically and experimentally, to rationalize and understand the consequences of the peculiar electronic structure of this class of open-shell systems.[23,50,53–57] SHI has been investigated in organic spin-polarized donor systems as a route toward high-spin diradicals,[18,58–62] and also in the case of luminescent radicals where SHI was associated with a significant increase of photostability.[38] Coote, Corminboeuf *et al.* summarized various theoretical aspects related to the characterization of this phenomenon with molecular examples of SHI in 2015.[50] Very recently, Abe *et al.* exhaustively surveyed the reported compounds in which SHI has been identified.[55] Given the strong attention that SHI organic radicals have received again recently, it appears timely to review the synthetic challenge to obtain SHI in open-shell compounds, as well as some important new theoretical insight regarding the occurrence of SHI and its impact on the molecular optoelectronic and magnetic properties.

In this short review, our objective is to give the readers a general perspective on SHI, with key fundamental aspects regarding the electronic and structural factors that govern this particular electronic configuration in organic radicals. We first introduce some basic considerations regarding SHI and explain why the 'non-*aufbau*' designation is somewhat imprecise in the context of spin-unrestricted SCF MO calculations. We then present the current theoretical understanding of the electronic factors that govern SHI in organic radicals, along with selected examples of reported compounds illustrating these findings. This is followed by a description of the common features exhibited by the SHI radicals reported in the literature, based on what is known about the key parameters responsible for SHI, along with a discussion of the (actual or postulated) consequences of this electronic configuration on the molecular properties of radicals, especially their (photo)stability. We hope that this work will not only provide a general view of the current state-of-the-art, but will also identify new opportunities for future research directions.

SOMO–HOMO inversion (SHI): basic considerations

Strictly speaking, the electron orbitals calculated for many-electron systems, and their energies, are not observable. However, the orbitals acquire meaning *via* approximations. For example, per Koopmans' theorem, the vertical ionization potential (IP) is up to a sign approximately equal to ε_H, with the latter being the HOMO energy from a Hartree–Fock (HF) calculation. Similarly, the LUMO is approximately associated with electron attachment (EA = electron affinity). In Kohn–Sham density functional theory (DFT), IP = $-\varepsilon_H$, holds exactly, as long as the functional is exact. This is often referred to as Janak's theorem; for a critique see ref. 63. In practice, with approximate functionals, DFT HOMO and LUMO energies may differ considerably, numerically, from the IP and EA, although procedures are available to establish these numerical relationships very closely.[64,65] Koopmans' and Janak's theorem and their relation to electron removal or addition are also fundamentally related to Fukui functions and associated concepts describing the reactivity of a molecule.[66] Therefore, as chemists know well, the orbitals of a molecule provide important qualitative, and sometimes even quantitative, information about its physicochemical properties. Regarding SHI, for a reliable assignment by calculations the presence or absence of SHI should be robust, *i.e.*, not sensitive to the chosen electronic structure approximations such as the functional used in DFT calculations.

As mentioned, SHI has been associated with a non-*aufbau* electronic configuration similar to what has been reported for metal complexes[67–69] and certain types of high-spin restricted open-shell HF calculations.[70] We reiterate that in spin-unrestricted MO theory, that is, in spin-unrestricted HF or DFT SCF calculations, matching α- and β-spin MOs may have different energies. 'Matching' means the spatial functions are the same, or very similar.† For the reported SHI molecules, the SUMO is above the HOMO in energy in such calculations.

† Spin-unrestricted SCF calculations may not always produce the SOMO and SUMO with obviously matching spatial functions, even if spin contamination is not severe. The orbitals produced by standard SCF calculations are called 'canonical'. We have previously noted cases where an α-spin SOMO matching the appearance of a β-spin SUMO was represented by a linear combination of occupied α-spin canonical MOs.

Therefore, there is no unoccupied spin orbital energetically below the highest occupied spin orbital, the *aufbau* rule is not technically violated, and the non-*aufbau* designation should probably be avoided unless there is actually a 'hole below the Fermi level'.[71] Nonetheless, of course, SHI is very intriguing. As depicted in Fig. 3, the general illustration of SHI is that the HOMO pair of matching spin orbitals is higher in energy than the SOMO, and below the corresponding β-spin hole represented by the SUMO.

This electronic configuration sets the electronic properties of these radicals apart from the more common situation where the SOMO is the highest occupied orbital of the system. While it is not always obvious to relate the electronic configuration of a molecule to its thermodynamic stability and other properties, what is clear is that when SHI is present, further oxidation of the molecular system will most likely produce an open-shell diradical instead of a closed-shell configuration. This is because, per Koopmans' or Janak's theorem, further ionization of the radical will be from its HOMO. This specific reactivity has been successfully used to produce an organic diradical with a triplet ground-state,[72] resulting from the oxidation of a monoradical with SHI electronic configuration (*vide infra*). Also, the energetic inversion of the SOMO and HOMO has been recently associated with a certain gain of chemical and/or photophysical stability for organic radicals,[73,74] thus potentially offering a complementary approach to the two classical ones for stabilizing radicals (*i.e.* shielding the unpaired electrons with bulky substituents, or enhancing their delocalization over the molecular backbone[10,11,75–79]). Complementing these molecular material applications, organic radicals with SHI have recently been claimed as key intermediates for regiospecific reaction of C(sp^3)H-amination and photocatalytic allylation, providing alternative directions for organic synthesis.[80,81]

Design strategies for SHI radicals

Numerous molecular systems have been reported to show SHI. However, a clear understanding of the electronic factors that lead to this specific electronic configuration has been lacking. Pioneering work related to this aspect started in the 90 s with the contributions of Sugimoto,[82] Sawaki[83] and Sugawara,[84–88] who explored SHI electronic configurations in organic compounds implying highly persistent and localized radicals. For instance, Sugawara and co-workers developed several molecular systems combining an electron donor unit and a pendent radical, named spin-polarized donor, with SHI configuration and potentially spin-polarized current conduction.[18] The investigated design of these compounds was mainly based on the nitronyl nitroxide radical unit functionalized by different organic electron donor fragments (Fig. 4), in a way that the two parts weakly interact electronically with each other. Based on a structure–properties relationship study, Sugawara *et al.* identified important structural and electronic factors that favor SHI in the spin-polarized donors, involving notably the electron donor strength of the fragment bearing the HOMO level, and the torsion angle between the latter and the radical unit (Fig. 4).

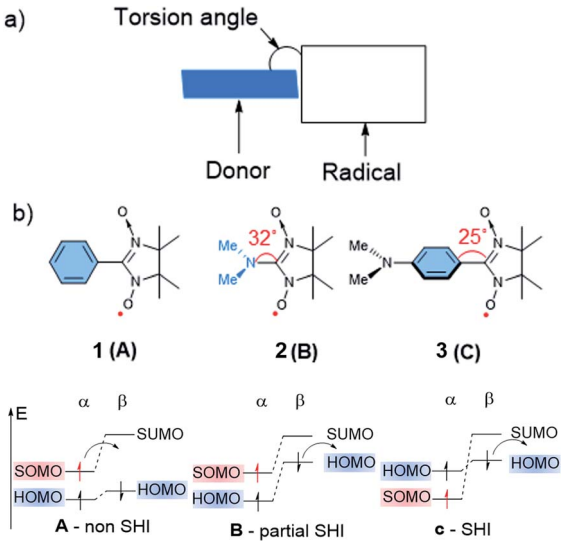

Fig. 4 (a) Schematic illustration of the Sugawara spin-polarized donor structure. (b) Nitronyl nitroxide radical **1**, **2**, and **3** with corresponding torsion angles between the radical and donor fragments in degrees with schematic illustration of the corresponding electronic configuration. Figures adapted with permission from ref. 59. Copyright 2000 American Chemical Society.

As illustrated in Fig. 4, three possible scenarios can be considered for these donor-radicals, resulting in different electronic configurations:[59]

- (A) When a weak electron donor unit is connected to the radical, such as for example a benzene unit in phenyl nitronyl nitroxide **1**, the α-SOMO is higher in energy than the HOMO, resulting in a common open-shell molecular orbital arrangement with the SOMO being the highest occupied orbital.

- (B) In the case of dimethylamino nitronyl nitroxide **2**, increasing the donor strength of the organic donor unit results in an α-SOMO that is higher in energy than the α-HOMO, but lower in energy than the β-HOMO. The energetic splitting between the α-HOMO and β-HOMO arises from a non-equivalent electronic repulsion between the latter two and the α-SOMO, as evidenced by spin-unrestricted calculations. Thus, this electronic configuration affords what we may call partial SHI, where oxidation would likely occur from the β-HOMO instead of the α-SOMO.

- (C) Decreasing the electronic interaction between the donor and radical units while keeping the donor strength character of the organic donor unit results in a complete SHI electron configuration, where both α- and β-HOMO energy levels become higher in energy than the α-SOMO. For instance, *p*-aminophenyl nitronyl nitroxide **3** displays this kind of electronic configuration.

Interestingly, the two latter types of design should give a diradical with a triplet ground-state upon one-electron oxidation of the donor unit in accordance with Hund's first rule, and because of the non-disjoint connection of the resulting two SOMOs, following Borden and Davidson.[89] Experimentally, this kind of specific reactivity can be characterized using

electrochemical methods, electron paramagnetic resonance (EPR) and magnetometry measurements (*vide infra*).

Having these preliminary molecular guidelines in mind, we recently embarked on a computational study with the aim of understanding the electronic factors that govern SHI in already reported mono-radicals. The findings were then applied to identify potential SHI candidates '*in silico*'.[53] Prior calculations already indicated that SHI might be less uncommon than once thought,[57] especially for small systems or spatially compact (localized) SOMOs, hinting at the important role of intra *vs.* inter-orbital electron repulsion discussed in the following. Analysis of various contributions to the MO energies individually, along with selected electron repulsion integrals (ERIs) for the frontier MOs, was carried out. The SHI analysis starts out with a closed-shell parent (CS), which is analogous to the radical but has one additional electron. Initially, the CS parent is in its equilibrium structure (CS//CS). The radical is then formed in three steps:

(i) Removal of an electron without letting the MOs or structure relax: CS//CS → R̃//CS.

(ii) MO relaxation *via* SCF: R̃//CS → R//CS.

(iii) The radical adopts its own equilibrium structure: R//CS → R//R.

Step (i) is key and typically already establishes SHI. Based on the analysis, the preconditions in the CS system for formation of an SHI radical are as follows: (a) the CS HOMO energy is balanced by a large self-Coulomb repulsion (*i.e.*, the repulsion between the α and β spin component of the HOMO) and a strongly stabilizing negative electron–nucleus attraction. The former can be tuned *via* the spatial compactness of the moiety on which the MO is localized, and the latter by inductive effects from substituents or substitution of carbon with electronegative heteroatoms, for example. As noted later, bonding *vs.* antibonding character of an MO may also be a factor in the energetic balance. (b) The HOMO self-Coulomb repulsion in the CS system is considerably larger than the repulsion between the HOMO and other occupied frontier orbitals (HOMO − 1, in particular). This is the reason why many of the known SHI radicals have spatially disjoint HOMO and SOMO: when the MOs are disjoint, their mutual Coulomb repulsion is relatively weak, favouring SHI in the presence of condition (a).

The main effect from removing an occupation from the CS HOMO, to form the radical, is then a strong stabilization of the orbital's remaining occupied spin component, from the loss of the self-Coulomb repulsion according to condition (a), whereas HOMO − 1 and potentially other occupied frontier MOs are far less stabilized because of condition (b). The SOMO ends up below one or several pairs of matching spin orbitals. The energy of the SUMO still contains the Coulomb repulsion with the SOMO, and therefore it remains high in energy.

In a nutshell, the formation of an SHI radical is likely to occur when the electrons in the HOMO of the CS parent repel each other strongly, while the repulsion between the HOMO and other occupied frontier MOs is much weaker. Then, the SHI is driven by the loss of a considerable amount of repulsive energy upon removing one of the HOMO occupations. In a design approach that starts with a radical moiety already, connecting the latter with an electron donor group that has a lower IP, while keeping the electronic interaction between the two units relatively weak, likewise seems to represent an efficient way of creating SHI radicals, as illustrated in Fig. 4.

A counter example of the crucial role of step (i) in establishing SHI is the case of a system composed of two identical fragments with limited electronic interaction, in which one fragment is then oxidized. A representative example of that system if the case of the bicarbazole radical cation **4**$^{\bullet+}$ (Fig. 5 and *vide infra*),[74] a system with a CS parent composed of two identical carbazole fragments, which we recently reported as the first enantiopure chiral SHI monoradical.[74] In the CS parent system, the HOMO and HOMO − 1 are essentially in-phase and out-of-phase (+/−) linear combinations of individual carbazole fragment frontier orbitals, with Coulomb ERIs within and between HOMO and HOMO − 1 being nearly the same. The vertical ionization of dimer **4** does not immediately afford an SHI system. For such a design and presumably related ones, such as in bridged bicarbazole radical cation **5**$^{\bullet+}$, a significant distortion of the molecular structure upon oxidation is required for the occurrence of SHI (step (ii) in Fig. 5a), causing the HOMO and SOMO to localize on separate fragments. Nonetheless, key to understand the occurrence of SHI in a radical is the electrostatic repulsion among the frontier orbitals, before and after the radical formation.

Another type of SHI radical can be also identified, in which the HOMO and SOMO are spatially overlapping. This scenario is exemplified by the radical aza-thia[7]helicene derivatives **6**$^{\bullet+}$

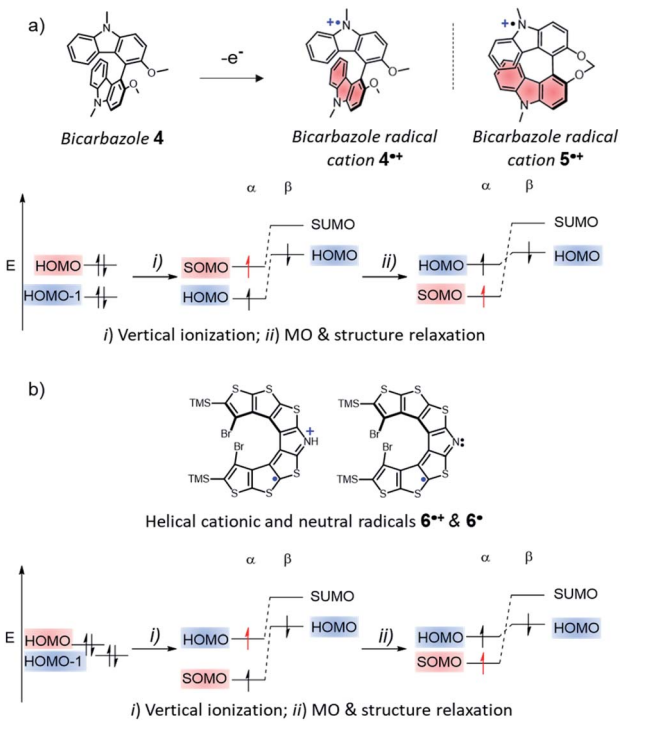

Fig. 5 Chemical structures of (a), the bicarbazole radical cations **4**$^{\bullet+}$ and **5**$^{\bullet+}$ and (b), the cationic radical aza-thia[7]helicene **6**$^{\bullet+}$ and neutral aza-thia[7]helicene **6**$^{\bullet}$, with a schematic illustration of the steps leading to SHI.

and **6**$^{\bullet}$ reported by Rajca *et al.* in 2016 (Fig. 5b and *vide infra*).[56] In this system, as revealed by our previous computational analysis, the HOMO and HOMO − 1 of the CS parent are effectively degenerate, and they both have strong—but sufficiently different—self-Coulomb repulsions. Moreover, there is a large Coulomb ERI between these two orbitals because they strongly overlap spatially. As for the SHI radical design mentioned first (Fig. 4), the ionization of the CS parent **6** induces the loss of a particularly large self-Coulomb ERI and results directly in SHI. Although significant orbital and structure relaxation also occurs, because of the spatial overlap of the HOMO and SOMO, the loss of the larger of the two Coulomb repulsion terms in the total energy favours the SHI ground-state configuration of the radical, and may likewise induce SHI in systems with similar orbital energetic characteristics.

To summarize thus far, calculations have uncovered electronic factors resulting in organic radicals with SHI and furthermore shown that the SOMO–HOMO energy gap in a multifragment SHI radical can be tuned *via* optimizing the HOMO energies of the precursor molecules (see ref. 53). While a clear molecular design to obtain SHI radical has been identified by the work of Sugawara *et al.*, the recent results obtained on bicarbazole and aza-thia[7]helicene derivatives indicate that other strategies may be also relevant to obtain SHI radicals. Accordingly, further investigations are currently needed to rationalize these new approaches and provide new molecular guideline strategies. In the following sections, we discuss selected examples of organic SHI radicals, in which some common features can be identified with the ones illustrated by these theoretical results.

(i) SHI radical with a radical fragment weakly interacting with an electron donor unit

As mentioned, one of the strategy to design SHI organic radical relies on the functionalization of a radical unit by a secondary electron donor unit with a lower ionization potential (IP) while ensuring spatially disjoint HOMO and SOMO.

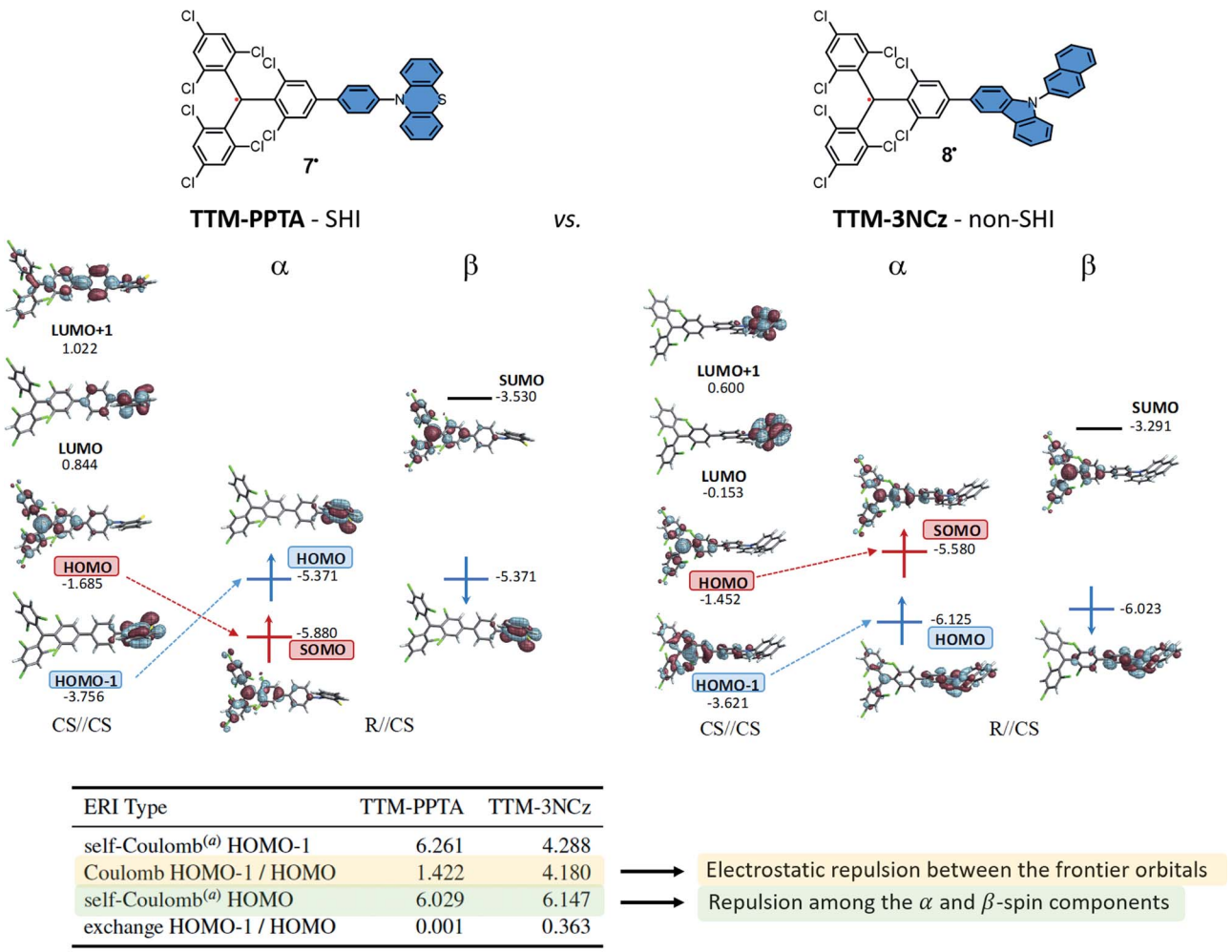

ERI Type	TTM-PPTA	TTM-3NCz
self-Coulomb[(a)] HOMO-1	6.261	4.288
Coulomb HOMO-1 / HOMO	1.422	4.180
self-Coulomb[(a)] HOMO	6.029	6.147
exchange HOMO-1 / HOMO	0.001	0.363

→ Electrostatic repulsion between the frontier orbitals
→ Repulsion among the α and β-spin components

Fig. 6 Orbital energies (in eV) and isosurfaces (0.030 a.u.) of selected MOs of the TTM−PPTA, **7** and TTM−3NCz, **8** systems. See the text for a description of the CS//CS and R//CS labelling. The vertical dimension of the figure is associated with the orbital energy; however, as in other figures herein, the energy scales are drawn qualitatively and are not aligned. The table provides selected Coulomb and exchange electron repulsion integrals (ERIs, in eV) for the corresponding closed-shell parent systems. [a]Coulomb repulsion between the α- and β-spin component of the MO. Figures adapted with permission from ref. 53. Copyright 2021 American Chemical Society.

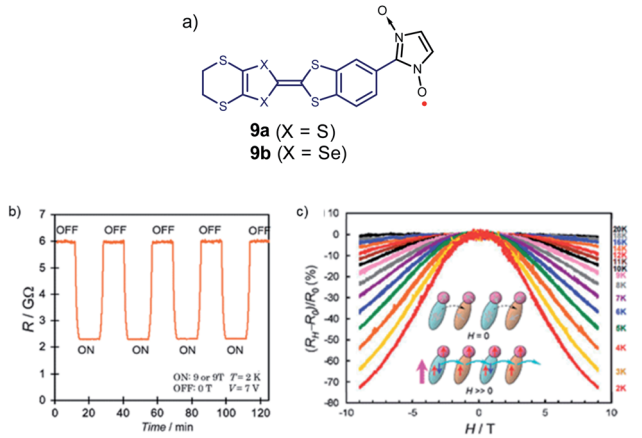

Fig. 7 (a) Example of spin-polarized donors **9** where both magnetic and spin conductivity properties co-exist. (b) Magnetic switching of resistance of **9b** at constant voltage. (c) Temperature-dependence of the ratio of magnetoresistance of **9b** at a bias voltage of 7 V. Reprinted figures with permission from ref. 101. Copyright 2008 by the American Physical Society.

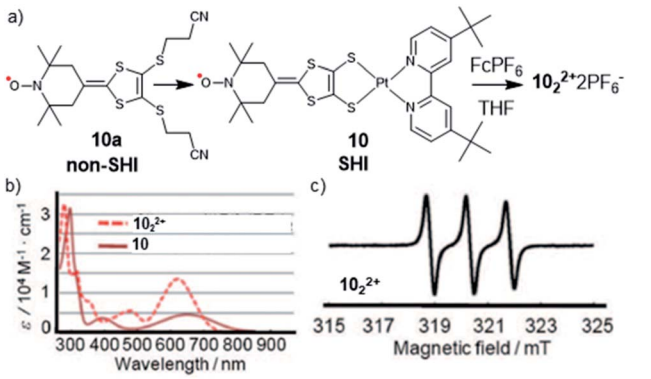

Fig. 8 (a) Molecular structures of radical ligand tempodt **10a**, platinum–tempodt complex **10**, with the formation of the dimerized complex $\mathbf{10}_2^{2+}$ and (b) the UV-vis spectra of **10** and $\mathbf{10}_2^{2+}$; (c) EPR spectrum of $\mathbf{10}_2^{2+}$. Figures adapted with permission from ref. 106. Copyright 2008 American Chemical Society.

An example of this design is detailed in Fig. 6 with compounds developed by Li, Brédas, Friend, and coworkers as doublet emitters for OLED applications.[38] The chemical structure of these neutral radicals are based on the known luminescent tris(2,4,6-trichlorophenyl)methyl (**TTM**) radical,[27,90,91] functionalized by either a phenyl-phenothiazine (**PPTA**) or a carbazole unit (**3NCz**) as donor groups. These organic neutral radicals can be readily prepared by one-electron oxidation of the corresponding anions, obtained *via* deprotonation of the hydrogenated precursors HTTM–**PPTA** and HTTM–**3NCz**, and represent an interesting comparison between a system with SHI (**TTM–PPTA**, 7) *vs.* without (**TTM–3NCz**, **8**).

Using cyclic voltammetry (CV), ultraviolet photoelectron spectroscopy (UPS), EPR and computational methods, it was shown that the SHI electronic configuration can be obtained when there is not too strong electronic coupling between the neutral radical and the electron donor unit, as already mentioned, which in some cases goes along with near-orthogonal conjugated π systems. Accordingly, in **TTM–PPTA** the SOMO remains mainly localized on the triphenylmethyl radical moiety, and lies below the HOMO found mostly on the phenothiazine fragment. For this molecular design, *i.e.* a persistent radical weakly interacting with an electron donor unit, SHI is typically established in step (i) in the theoretical analysis (*vide supra*). As depicted in Fig. 6, both the release of the energetic repulsion between the α- and β-spin components of the HOMO in the CS of **TTM–PPTA** and the limited electrostatic repulsion between HOMO and HOMO − 1 are the key factors to obtain SHI. For **TTM–3NCz**, the stronger electronic interaction between the HOMO and HOMO − 1 disfavors the occurrence of SHI and ultimately leads to a classical organic radical electron configuration, with the SOMO higher in energy than the HOMO.

Another interesting finding of Li, Brédas, Friend, *et al.* was that the photostability of the luminescent radical with SHI was nearly five orders of magnitude higher than of **PTM** alone, and up to four orders of magnitude higher than similar radical derivatives without SHI reported in the literature.[17,38] This effect was attributed to the SHI as well as the charge-transfer nature of the excited-state of the radical promoted by the presence of the carbazole unit, limiting some photodegradation reactions.

As already discussed, Sugawara *et al.* applied this strategy to construct a variety of spin-polarized donors based on amino groups, pyrrole, and other tetrathiafulvalene derivatives,[61,92–104] and showed that this type of compounds can exhibit coexisting conductivity and magnetism, as illustrated with molecules **9a**, **b**, resulting from a combination of the bis-ethylenedithiotetraselenafulvalene (ESBN) donor and the nitronyl nitroxide (NN) radical (Fig. 7).[72,101,105]

In 2008, Nishihara *et al.* found that SHI can also be induced in organometallic complexes, by using the coordination of a platinum(II) ion by a dithiolate organic radical ligand (tempodt **10a**, Fig. 8).[106] Whereas the latter, composed of a (2,2,6,6-tetramethylpiperidin-1-yl)oxyl (TEMPO) fragment, displays the SOMO as its highest occupied orbital, Pt(II) complex **10**, with 4,4′-di-*tert*-butyl-2,2′-bipyridyl as the ancillary ligand, shows an SHI configuration. The authors attributed this effect to an antibonding interaction of the highest doubly occupied MO of the tempodt ligand and the HOMO of Pt(*t*Bubpy)$^{2+}$, which raises the energy of the resulting HOMO in complex **10** above the SOMO. Furthermore, strong on-site Coulomb repulsion of the SOMO and its weak interaction with the HOMO, exclusively localized on the dithiolate ligand, were considered as decisive factors in obtaining SHI. These conclusions were supported by

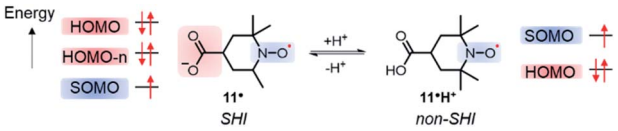

Fig. 9 Molecular orbital configurations of the carboxy-aminoxyl radical in both anionic $\mathbf{11}^{\bullet}$ and neutral $\mathbf{11H}^{+}$ forms.

CV measurements, UV-vis spectroscopy, EPR, and DFT calculations. Interestingly, oxidation of the complex using the ferrocenium chemical oxidant resulted in the formation of dimer $\mathbf{10_2 \cdot 2PF_6}$ (Fig. 8). A clear triplet signal in the ESR spectrum, arising from the hyperfine coupling between the radical center and the nitrogen nucleus, indicated the presence of a nitroxide radical within the dimeric product, confirming that the removal of the electron involves the HOMO and not the SOMO of the complex. Nishihara *et al.* further investigated this approach using different metal ions such as nickel(II), gold(I), and palladium(II),[107–109] likewise showing SHI electron configurations.

Following a similar direction, Coote *et al.* highlighted a potential consequence of SHI on the resulting chemical stability of the radical.[110] The authors used distonic radical anions based on either stable diallyl or nitroxide radical units, linked *via* sigma bonds to a carboxylate group in which the HOMO has higher energy than the radical's SOMO (Fig. 9). Based on experimental and theoretical evidence, the authors found that the anion stabilizes the radical moiety and that the electronic configuration can be switched between *aufbau* and non-*aufbau* by protonation of the anionic group (Fig. 9). It was furthermore suggested that such a mechanism of stabilization also operates in nucleic acid radicals because of the presence of sulfate and phosphate groups, thus preventing undesirable radical reactivity.

Coote *et al.* expanded their investigations to other distonic radical anions and found that the stabilization effect diminishes in polar solvents,[111] and even disappears in water, as also experimentally confirmed a year later by Lucarini *et al.* using bond dissociation energy measurments.[112]

In 2019, Kusamoto, Nishihara *et al.* reported another example of an SHI radical showing the radical site switching with the acidity of the medium,[113] based on a similar molecular design as the radical emitters developed by Friend, Brédas and Li *et al.* (Fig. 6),[38] *i.e.*, a donor–acceptor radical, using triphenylamine (TPA) as the electron donating unit and a molecular analogue of the **TTM** radical with the phenyl ring replaced by 3,5-dichloro-4-pyridyl (**12**, Fig. 10). In neutral conditions, **12** shows SHI with the SOMO being located mainly on the triaryl radical unit and the HOMO localized on the triaryl amine donor fragment, as shown by DFT calculations. Upon titration with

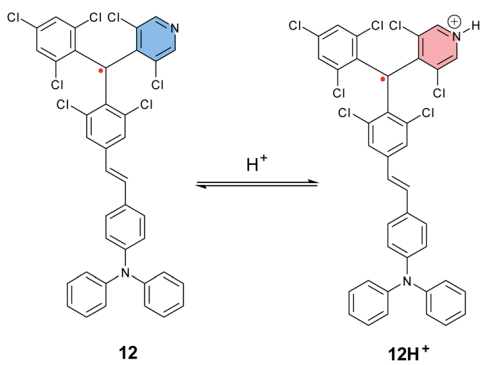

Fig. 10 Molecular structures of tris(2,4,6-trichlorophenyl)-methyl radical, PyBTM **12**, and [TPA–RH$^+$]$^\bullet$, **12H$^+$**.

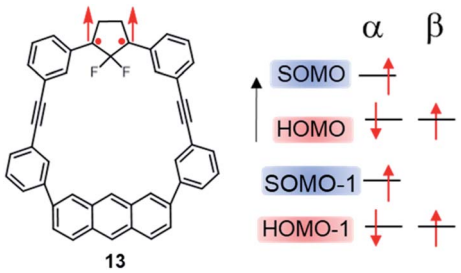

Fig. 11 Molecular structure of triplet ground state cyclopentane-1,3-diyl diradical **13** within a π-conjugated macrocycle, exhibiting partial SHI in the sense that the SOMO − 1 is below a doubly occupied MO while the SOMO remains the highest energy level.

trifluoroacetic acid (or with $B(C_6F_5)_5$ as a lewis acid), protonation of the pyridine moiety occurs and induces an increase of the intramolecular charge transfer (ICT) occurring from the neutral donor to the radical unit. This results in a significant bathochromic shift in the UV-vis-IR absorption spectrum, as well as quenching of the radical luminescence, while keeping the SHI electron configuration. Moreover, an excess of acid (>200 eq.) triggers an intramolecular electron transfer from the trisarylamine to the radical center, affording a possibility to switch between TPA–[RH]$^{\bullet+}$ and [TPA]$^{\bullet+}$–RH.

More recently, Abe, *et al.* investigated theoretically the electron configurations of diradical compounds based on a macrocycle composed of an anthracene and a 2,2-difluorocyclopentane diradical unit, linked together by two diphenylethyne fragments (**13**, Fig. 11).[114,115] In this molecule, the HOMO is mainly localized on the anthracyl unit, with little electronic interaction with the SOMO and SOMO − 1 found on the 1,3-diphenylcyclopentane. Both the presence of the anthracene fragment and fluorine atoms within the cyclopentane unit were shown to be important factors to establish SHI, by raising the energy of the HOMO and stabilizing the SOMO and SOMO − 1, respectively.

(ii) SHI radicals from symmetric dimer compounds

While the SHI concept has been popularized in the last decade (with the term of spin-polarized donor, *vide supra*), it is important to mention the work of Kinoshita *et al.* reported in 1987, on the galvinoxyl radical **14** (Fig. 12).[116] Interested in the possibility of designing intermolecular ferromagnetism in organic materials, the team studied the orbital energies of the galvinoxyl radical using spin-unrestricted calculations and demonstrated that partial SHI occurs in the system, attributed

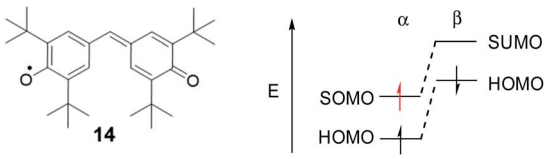

Fig. 12 Chemical structure of galvinoxyl radical **14** and its simplified orbital energy diagram.

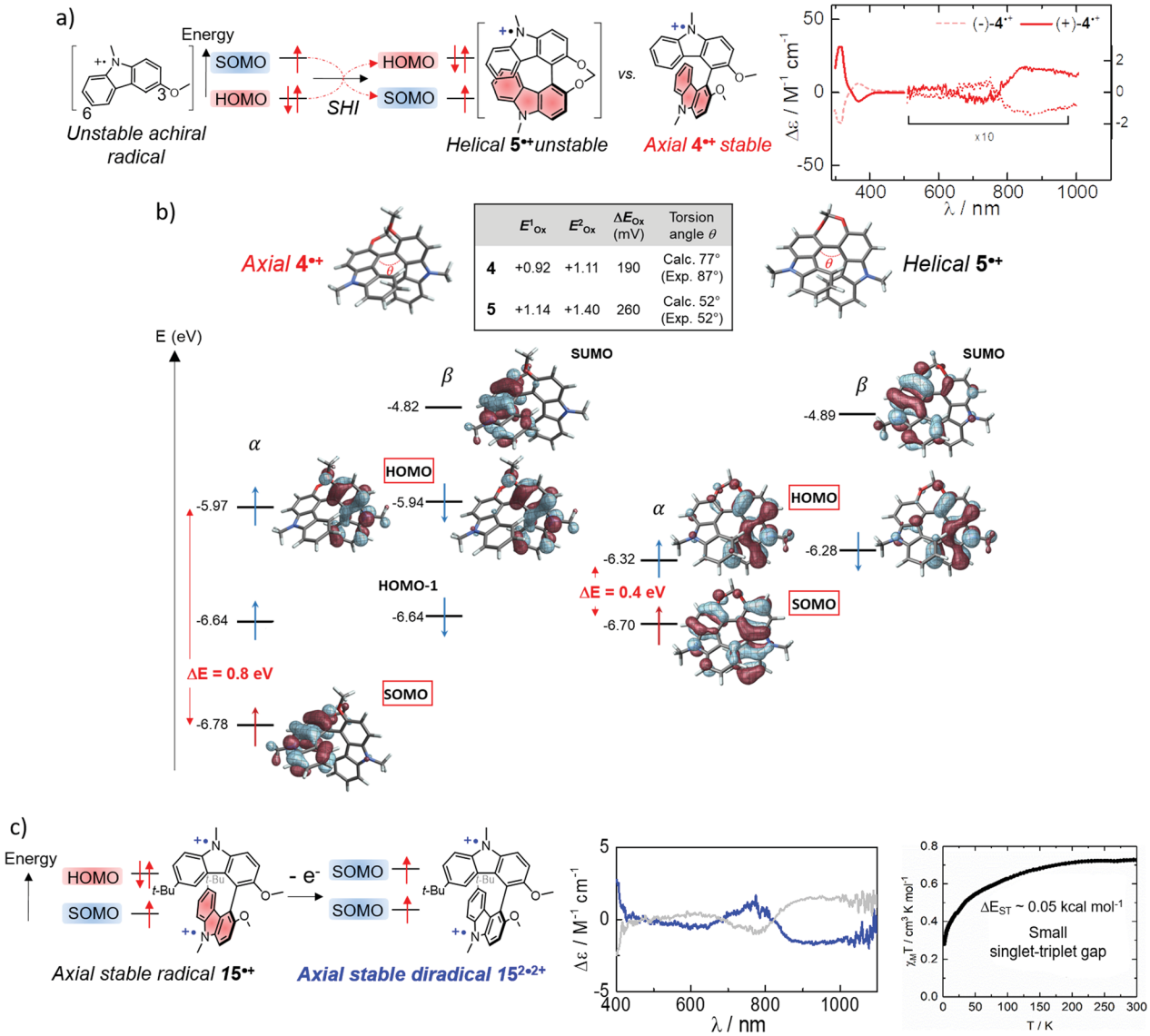

	E^1_{Ox}	E^2_{Ox}	ΔE_{Ox} (mV)	Torsion angle θ
4	+0.92	+1.11	190	Calc. 77° (Exp. 87°)
5	+1.14	+1.40	260	Calc. 52° (Exp. 52°)

Fig. 13 (a) Axially and helically chiral SHI cationic bicarbazole monoradicals $4^{\bullet+}$ and $5^{\bullet+}$, and orbital comparison with their common non-SHI cationic carbazole radical precursor, with the near IR circular dichroism of (+) and (−)-$4^{\bullet+}$ (counter anions are omitted for clarity); (b) calculated orbital energies (in eV) and isosurfaces (±0.030) of frontier molecular orbitals computed for monoradicals $4^{\bullet+}$ (left) and $5^{\bullet+}$ (right). The HOMO–SOMO energy differences are averaged over the highest occupied spin orbital energies. Oxidation potentials and separation of the two first oxidation potentials in *V vs.* SCE, theoretical (calc.) and experimental (exp.) dihedral angles between the carbazole fragments; (c) schematic illustration of the electronic configuration of diradical $15^{2\bullet 2+}$ obtained upon oxidation of SHI radical $15^{\bullet+}$, near IR circular dichroism of (+) and (−)-$15^{2\bullet 2+}$ in acetonitrile at 298 K, and its magnetic susceptibility ($\chi_M T$ *vs.* *T*). Figures adapted with permission from ref. 74. Copyright 2020 American Chemical Society.

to a difference of spin polarisation of the α and β spin component of the HOMO. These results also suggested that the oxidation of a radical with this kind of electronic configuration may favor the formation of a triplet diradical by selective oxidation involving the β-spin component of the HOMO.[117–119]

Compound **14** can be therefore considered as an SHI precursor, based on a molecular dimer design, which has been mentioned already in the context of bicarbazole radical cations $4^{\bullet+}$ and $5^{\bullet+}$ (Fig. 5 and 13).[74] The investigation of these radical systems allowed us to explore the SHI in chiral radical molecular systems and provide new insights regarding its impact on the stability of organic radicals. Photophysical (UV-vis-NIR absorption), chiroptical (ECD, electronic circular dichroism) and electrochemical characterization of the neutral bicarbazole system and its radical cationic form revealed high chemical stability for unprotected carbazole axial radical $4^{\bullet+}$, in comparison to unstable helical $5^{\bullet+}$, and in striking contradiction to the known polymerization reactivity of unprotected oxidized carbazole in the 3 and 6 positions (Fig. 13).[120] Interestingly, both $4^{\bullet+}$ and $5^{\bullet+}$ exhibit SHI, indicating that such an electronic configuration is not a sufficient prerequisite to provide radical stability. Our experimental and theoretical results rather

suggest that in addition to SHI, the electronic coupling between the radical center and the electron-rich unit on which the HOMO is centered plays a crucial role in the radical reactivity. In $\mathbf{4}^{\bullet+}$ and $\mathbf{5}^{\bullet+}$, this aspect depends on the dihedral angle between the carbazole moieties, which is governed by the axial and helical chirality of the bicarbazole systems.

Furthermore, the persistence of $\mathbf{4}^{\bullet+}$ provided an interesting opportunity to generate the corresponding chiral diradical. Oxidation of the remaining HOMO of sterically protected monoradical $\mathbf{15}^{\bullet+}$ gave chiral diradical $\mathbf{15}^{2\bullet2+}$ with intense near-infrared (NIR) circular dichroism (Fig. 13). The radical's ground-state spin multiplicity appeared to be the low-spin singlet. This result was theoretically rationalized by a relatively weak interaction between the two SOMOs being each localized on one carbazole unit and ultimately favoring the singlet ground state. This work represents one of the rare examples of organic chiral radicals displaying SHI in which the corresponding chiroptical properties have also been investigated.

With the growing interest in chirality as a property of molecular materials,[121–125] it has recently emerged that combining the attractive electronic/spin properties of an organic radical with a chiral organic π-conjugated system may give rise to molecular architectures with unique magnetic and chiroptic-electronic features, such as absorption of near infrared (NIR) circularly polarized (CP) light,[56,79,126–134] radical CP luminescence (CPL),[135,136] and possibly enhanced spin-filtering properties.[137] However, designing organic chiral open-shell chromophores remains a formidable challenge, owing to the aforementioned high chemical reactivity and poor configurational stability that is typical of radicals.[138] As for achiral radical systems, shielding the unpaired electrons with bulky substituents, or enhancing their delocalization over the molecular backbone have been used to overcome these issues.[10,11,75–79] While these approaches can be efficient, they often require additional synthetic steps and may preclude significant interaction between the unpaired electron and the chiral molecular system, thus precluding efficient intermolecular interactions

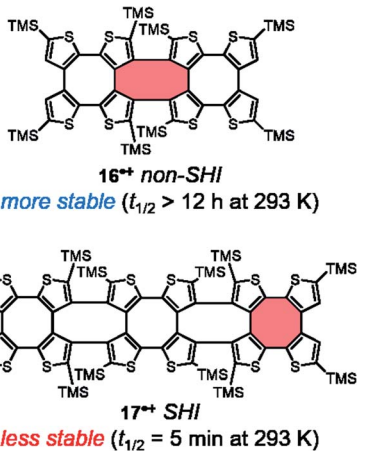

Fig. 14 Chemical structures of thiophene-based double helix radicals **16** and $\mathbf{17}^{\bullet+}$ (TMS = trimethylsilyl). The molecular fragment in red highlights the predominant localization of the SOMO within the molecular structure.

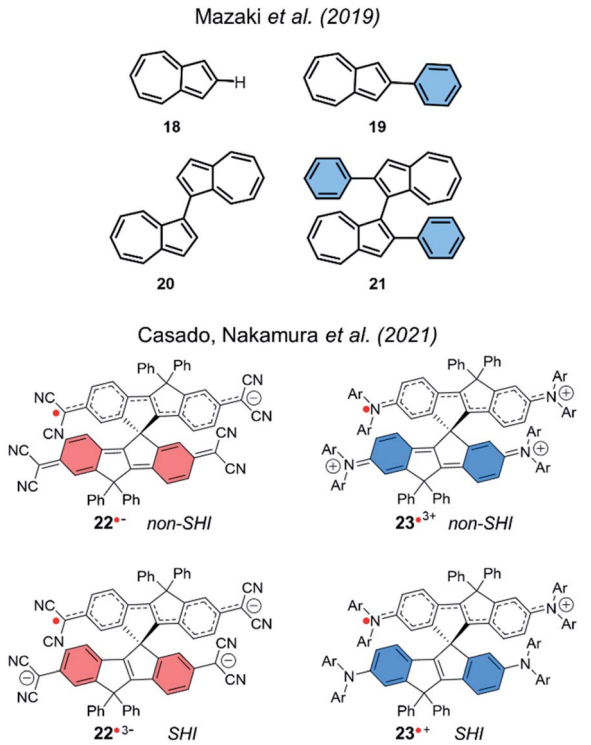

Fig. 15 Azulenes **18**–**19** and dimers of azulene **20**–**21** (top), and spiroconjugated systems **22**–**23** (bottom).

for charge and spin transport applications.[19] In this context, the design of atropisomeric systems such as the C_2-symmetric bicarbazole one depicted in Fig. 13 represents a potential strategy to obtain persistent and configurationally stable chiral radical. It is however important to note that some of the other SHI radicals described in this review are also chiral, such as the **PTM** and **PTM** derivatives, albeit without sufficient configurational stability at room temperature.[136]

Although no chiroptical properties were reported for the radicals thiophene-based double helices **16** and **17**, developed by Rajca *et al.* in 2021, they also represent interesting examples of chiral radicals of the symmetric-dimer type, in which SHI is present only for radical cation $\mathbf{17}^{\bullet+}$ (Fig. 14).[139,140] The cationic monoradicals $\mathbf{16}^{\bullet+}$ and $\mathbf{17}^{\bullet+}$ showed high persistence at 193 K (half-lives exceeding 24 hours). However, at room temperature in dichloromethane solution, radical $\mathbf{17}^{\bullet+}$ showed much less stability than $\mathbf{16}^{\bullet+}$ ($t_{1/2}$ < 5 minutes *vs.* >12 hours in $\mathbf{17}^{\bullet+}$). This result is in contradiction with the aforementioned findings for SHI *vs.* non-SHI radicals in terms of stability.[38,74,110] The authors of ref. 140 therefore suggested that the steric hindrance brought by the peripheral TMS-thiophene units in $\mathbf{16}^{\bullet+}$ plays a decisive role in stabilizing the unpaired electron. In fact, the spin density in $\mathbf{16}^{\bullet+}$ is mostly localized in the center of the molecule whereas for $\mathbf{17}^{\bullet+}$, it is also delocalized in the peripherical thiophene fragments (highlighted in red, Fig. 14).

SHI in a dimer molecular design was also theoretically investigated in cationic azulene radical by Mazaki *et al.* in 2019,[141] and more recently by Casado, Nakamura *et al.* in 2021.[23] Interestingly, in the latter report, the authors explored spiro-

conjugated systems with the ability to adopt SHI in both anionic and cationic radical forms (Fig. 15).

Using UV-vis-NIR absorption spectroscopy and DFT calculations, the team characterized a SHI for the radical trisanion of the quinoidal derivative $\mathbf{22}^{\bullet 3-}$ and for the radical cation $\mathbf{23}^{\bullet +}$. This report highlights a new design strategy for obtaining SHI open-shell systems based on spiro-conjugation and spiro-functionalization.

(iii) SHI radicals with spatially overlapping HOMO and SOMO

The first aza-thia[7]helicene radicals displaying SHI, $\mathbf{6}^{\bullet}$ and $\mathbf{6}^{\bullet+}[PF_6]^-$, represent interesting examples of this class of open-shell systems. Here, the HOMO and SOMO strongly overlap spatially (Fig. 16). Nonetheless, the difference in the intra- *vs.* inter-orbital repulsion upon formation of the radical must also be considered as the determining factor to favor the SHI electronic configuration in the radical (*vide supra*).

Following previous work on thia[7]helicene $\mathbf{24}^{\bullet+}$,[142] Rajca *et al.* replaced the central thiophene ring by a pyrrole unit, for the potential generation of helical nitrogen-centered neutral and cationic radicals, $\mathbf{6}^{\bullet}$ and $\mathbf{6}^{\bullet+}[PF_6]^-$, respectively (Fig. 16). Starting from the NH precursor, the corresponding radical cation, $\mathbf{6}^{\bullet+}[PF_6]^-$ was generated using a chemical oxidant in dichloromethane solution at low temperature (233 K). EPR measurements confirmed the open-shell electron configuration, with a broad $I = 1$ triplet with ^{14}N-hyperfine splitting, $a_N = 0.23$ mT, and isotropic $g = 2.005$. The team also generated the neutral aminyl radical $\mathbf{6}^{\bullet}$, either by oxidizing the anion precursor, or *via* an *in situ* deprotonation of the NH group of $\mathbf{6}^{\bullet+}[PF_6]^-$ using an inorganic base. The half-lives of these radicals were characterized in a mixture of dichloromethane/acetonitrile, reaching up to 8 h at 293 K. Based on cyclic voltammetry experiments and DFT calculations, Rajca *et al.* showed that for both radicals the SOMO is energetically below the HOMO, and that SHI can be maintained even in polar solvents such as dimethyl sulfoxide and water, in contrast with previous cases reported by Coote and Lucarini.[111,112]

Interestingly, the thia[7]helicene radical $\mathbf{24}^{\bullet+}[PF_6]^-$ without SHI has a weaker persistence with a half-life of ~15–20 min at room temperature, showing the importance of the pyrrole ring in **6** for increasing the stability of the corresponding neutral and cationic open-shell compounds. While a significant racemization barrier of about 35 kcal mol^{-1} was determined by DFT calculations, no chiroptical properties of this chiral organic radical were reported.[56]

In 2021, Abe, Antol, *et al.* reported another example of this type of molecular design, based on carbene derivatives displaying SHI.[54] Based on theoretical calculations, it was shown that triplet carbenes included in a cycloparaphenylene (CPP) scaffold have SOMO energy levels below the HOMO of the CPP ring (Fig. 17). This electronic configuration is found for the ring

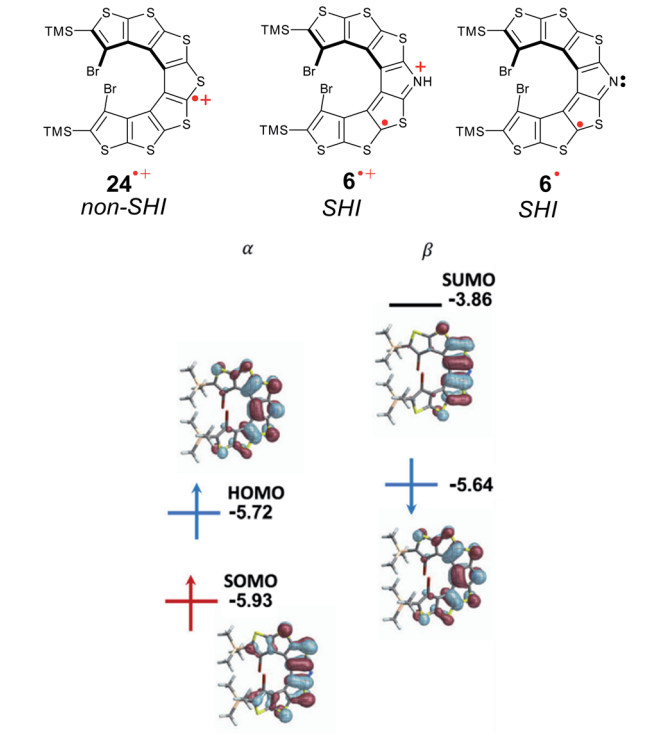

Fig. 16 Chemical structures of cationic radicals thia[7]helicene $\mathbf{24}^{\bullet+}[PF_6]^-$ and aza-thia[7]helicene $\mathbf{6}^{\bullet+}[PF_6]^-$, and neutral aza-thia[7]helicene $\mathbf{6}^{\bullet}$. Orbital energies (in eV) and isosurfaces (±0.030 a.u.) of selected MOs of $\mathbf{7}^{\bullet}$. Figures adapted with permission from ref. 53. Copyright 2021 American Chemical Society.

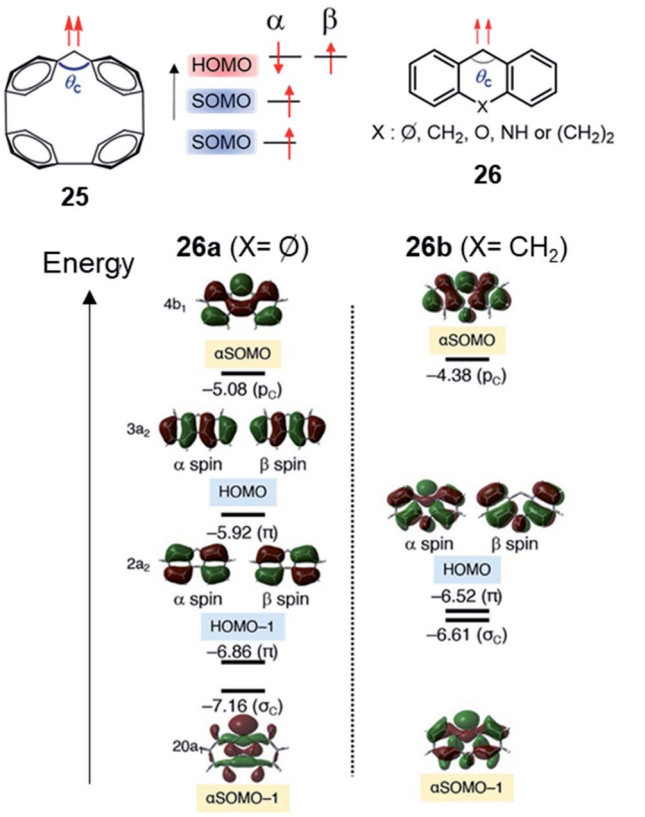

Fig. 17 Top: triplet carbenes included in a cycloparaphenylene (CPP) scaffold **25** and 2,2-difluorocyclopentane diradical **26** (left) showing SHI; with corresponding molecular orbital diagrams for **26a** and **26b**. Figure reprinted with permission from ref. 54. Copyright 2021 by the American Chemical Society.

composed of four phenyl units (**25**), whereas in larger carbene-CPP derivatives (5 to 10 phenyl units), the HOMO lies energetically in between the two SOMOs. This inversion, upon increasing the ring size, was explained by a simultaneous destabilization of the HOMO localized on the π-orbitals of the CPP ring and a stabilization of the SOMO within the σ-orbital of the carbene *via* an increase of the carbene angle, θ_c (Fig. 17). SHI also occurs in simpler carbenes such as **26**. The two aromatic rings stabilizing the carbene unit are structurally constrained, confirming the importance of the carbene angle (θ_c, Fig. 17). This result is particularly interesting given the extensive research on carbene chemistry, ranging from reactive intermediates to catalysis and material applications.

Conclusions and outlook

In this review, we have described a specific class of organic radicals, showing an energetic inversion of the singly occupied molecular orbital (SOMO) and the highest doubly occupied molecular orbital (HOMO), namely organic SHI radicals. We first discussed the basic features of organic radicals in terms of electronic structure, stability, optical, and photophysical properties, related to the presence of an unpaired electron. We then focused the discussion on SHI organic radicals and gave some considerations regarding this particular electronic configuration in relation to the *aufbau* rule. We also discussed several examples of organic SHI radicals based on neutral nitroxide, triphenylmethyl and carbene units, cationic carbazole derivatives and anionic spiroconjugated systems, and described structural and electronic design rules that govern the occurrence of SHI. Along with experimental evidence, theory has brought important insights regarding the key parameters leading to SHI, for example in terms of the electrostatic repulsion among the frontier orbitals and between the α and β spin components of a given MO.

This review also highlighted various specific features of SHI organic radicals, such as the postulated relationship between SHI and thermodynamic stability or photostability, which remains to be proven conclusively. The degree of 'energetic isolation' of the unpaired orbital in SHI radicals, when it is below the HOMO, means the HOMO instead of the SOMO defines the Fukui reactivity function in leading order. This opens the opportunity to relate electronic structure and reactivity directly with the SHI character of a system. Moreover, SHI radicals can be viewed as promising intermediates to form triplet ground state diradicals upon further oxidation of the HOMO level.

Merging the peculiar features of radical compounds and SHI with a chiral π-conjugated system is also currently attracting interest because of the potential of designing specific interactions with circularly polarized (CP) light[143–145] as well as magneto-chiral effects[146,147] and in the context of the chirality-induced-spin-selectivity.[148–150]

All these aspects appear particularly relevant for designing organic molecular materials with tailored spin properties, which are of high fundamental interest and may eventually offer new opportunities in organic spintronic and optoelectronic applications, both as semi-conductors,[18,19] or as efficient radical emitters.[27,38]

Fundamental questions remain yet to be fully addressed, notably regarding the relationships between SHI and radical stability, as well as other desirable radical properties that are not present in classical organic radicals. Future joined experimental and theoretical works will be aimed at teasing out these differences. We hope that this review highlights new opportunities for future research directions in organic radicals.

Author contributions

JA and LF co-wrote the manuscript and conceived the theoretical and experimental studies underlying a subset of the findings reported in the article, with comments and advices from JC. SK and LA designed figures and performed original research reviewed herein.

Conflicts of interest

There are no conflicts to declare.

Acknowledgements

L. F. and J. C. acknowledge the Ministère de l'Enseignement supérieur, de la Recherche et de l'Innovation, the Centre National de la Recherche Scientifique (CNRS). L. F. thanks the French National Research Agency (ANR, OChiRaLec project, ANR-21-CE07-0019-01) and the European Research Council (ERC, grant agreement number: 101041516—SHIFUMI—ERC starting grant (StG)) for financial support. J. A. thanks the National Science Foundation (CHE-1855470) for financial support of the theoretical component of our joint research.

Notes and references

1 J. H. Ardenkjær-Larsen, B. Fridlund, A. Gram, G. Hansson, L. Hansson, M. H. Lerche, R. Servin, M. Thaning and K. Golman, *Proc. Natl. Acad. Sci. U. S. A.*, 2003, **100**, 10158–10163.
2 B. B. Williams and H. J. Halpern, *Biomedical EPR – Part A: Free Radicals, Metals, Medicine and Physiology*, Springer US, 2005.
3 G. Mathies, M. A. Caporini, V. K. Michaelis, Y. Liu, K.-N. Hu, D. Mance, J. L. Zweier, M. Rosay, M. Baldus and R. G. Griffin, *Angew. Chem., Int. Ed.*, 2015, **54**, 11770–11774.
4 Z. Zeng, X. Shi, C. Chi, J. T. L. Navarrete, J. Casado and J. Wu, *Chem. Soc. Rev.*, 2015, **44**, 6578–6596.
5 Z. X. Chen, Y. Li and F. Huang, *Chem*, 2021, **7**, 288–332.
6 G. E. Rudebusch, J. L. Zafra, K. Jorner, K. Fukuda, J. L. Marshall, I. Arrechea-Marcos, G. L. Espejo, R. Ponce Ortiz, C. J. Gómez-García, L. N. Zakharov, M. Nakano, H. Ottosson, J. Casado and M. M. Haley, *Nat. Chem.*, 2016, **8**, 753–759.
7 M. Abe, *Chem. Rev.*, 2013, **113**, 7011–7088.
8 S. Kumar, Y. Kumar, S. K. Keshri and P. Mukhopadhyay, *Magnetochemistry*, 2016, **2**, 42.

9 X. Hu, W. Wang, D. Wang and Y. Zheng, *J. Mater. Chem. C*, 2018, **6**, 11232–11242.
10 T. Y. Gopalakrishna, W. Zeng, X. Lu and J. Wu, *Chem. Commun.*, 2018, **54**, 2186–2199.
11 K. Kato and A. Osuka, *Angew. Chem., Int. Ed.*, 2019, **58**, 8978–8986.
12 Y. Ni, T. Y. Gopalakrishna, H. Phan, T. Kim, T. S. Herng, Y. Han, T. Tao, J. Ding, D. Kim and J. Wu, *Nat. Chem.*, 2020, **12**, 242–248.
13 C. Liu, Y. Ni, X. Lu, G. Li and J. Wu, *Acc. Chem. Res.*, 2019, **52**, 2309–2321.
14 Q. Peng, A. Obolda, M. Zhang and F. Li, *Angew. Chem., Int. Ed.*, 2015, **54**, 7091–7095.
15 X. Gu, T. Y. Gopalakrishna, H. Phan, Y. Ni, T. S. Herng, J. Ding and J. Wu, *Angew. Chem., Int. Ed.*, 2017, **56**, 15383–15387.
16 X. Ai, Y. Chen, Y. Feng and F. Li, *Angew. Chem., Int. Ed.*, 2018, **57**, 2869–2873.
17 X. Ai, E. W. Evans, S. Dong, A. J. Gillett, H. Guo, Y. Chen, T. J. H. Hele, R. H. Friend and F. Li, *Nature*, 2018, **563**, 536–540.
18 T. Sugawara and M. M. Matsushita, *J. Mater. Chem.*, 2009, **19**, 1738–1753.
19 T. Sugawara, H. Komatsu and K. Suzuki, *Chem. Soc. Rev.*, 2011, **40**, 3105–3118.
20 D. Yuan, W. Liu and X. Zhu, *Chem*, 2021, **7**, 333–357.
21 Y. Tan, N. C. Casetti, B. W. Boudouris and B. M. Savoie, *J. Am. Chem. Soc.*, 2021, **143**, 11994–12002.
22 S. Kimura, R. Matsuoka, S. Kimura, H. Nishihara and T. Kusamoto, *J. Am. Chem. Soc.*, 2021, **143**, 5610–5615.
23 S. M. Rivero, R. Shang, H. Hamada, Q. Yan, H. Tsuji, E. Nakamura and J. Casado, *Bull. Chem. Soc. Jpn.*, 2021, **94**, 989–996.
24 I. Ratera, J. Vidal-Gancedo, D. Maspoch, S. T. Bromley, N. Crivillers and M. Mas-Torrent, *J. Mater. Chem. C*, 2021, **9**, 10610–10623.
25 C. Shu, M. Pink, T. Junghoefer, E. Nadler, S. Rajca, M. B. Casu and A. Rajca, *J. Am. Chem. Soc.*, 2021, **143**, 5508–5518.
26 A. Calzolari, A. Rajca and M. B. Casu, *J. Mater. Chem. C*, 2021, **9**, 10787–10793.
27 J. M. Hudson, T. J. H. Hele and E. W. Evans, *J. Appl. Phys.*, 2021, **129**, 180901.
28 Y. Teki, *Chem.–Eur. J.*, 2020, **26**, 980–996.
29 Y. Ni and J. Wu, *Tetrahedron Lett.*, 2016, **57**, 5426–5434.
30 J. Autschbach, *Quantum Theory for Chemical Applications: From Basic Concepts to Advanced Topics*, Oxford University Press, 2020.
31 L. K. Montgomery, J. C. Huffman, E. A. Jurczak and M. P. Grendze, *J. Am. Chem. Soc.*, 1986, **108**, 6004–6011.
32 J. Thiele and H. Balhorn, *Ber. Dtsch. Chem. Ges.*, 1904, **37**, 1463–1470.
33 A. E. Chichibabin, *Chem. Ber.*, 1907, **40**, 1810.
34 D. Griller and K. U. Ingold, *Acc. Chem. Res.*, 1976, **9**, 13–19.
35 S. Sowndarya S. V., P. C. S. John and R. S. Paton, *Chem. Sci.*, 2021, **12**, 13158–13166.
36 X. K. Chen, D. Kim and J. L. Bredas, *Acc. Chem. Res.*, 2018, **51**, 2215–2224.
37 M. Godumala, S. Choi, M. J. Cho and D. H. Choi, *J. Mater. Chem. C*, 2019, **7**, 2172–2198.
38 H. Guo, Q. Peng, X.-K. Chen, Q. Gu, S. Dong, E. W. Evans, A. J. Gillett, X. Ai, M. Zhang, D. Credgington, V. Coropceanu, R. H. Friend, J.-L. Brédas and F. Li, *Nat. Mater.*, 2019, **18**, 977–984.
39 A. Abdurahman, T. J. H. Hele, Q. Gu, J. Zhang, Q. Peng, M. Zhang, R. H. Friend, F. Li and E. W. Evans, *Nat. Mater.*, 2020, **19**, 1224–1229.
40 Y. Teki, *Chem.–Eur. J.*, 2020, **26**, 980–996.
41 K. Kato, S. Kimura, T. Kusamoto, H. Nishihara and Y. Teki, *Angew. Chem., Int. Ed.*, 2019, **58**, 2606–2611.
42 X. Liang, Z. L. Tu and Y. X. Zheng, *Chem.–Eur. J.*, 2019, **25**, 5623–5642.
43 Y. Liu, C. Li, Z. Ren, S. Yan and M. R. Bryce, *Nat. Rev. Mater.*, 2018, **3**, 18020.
44 H. Uoyama, K. Goushi, K. Shizu, H. Nomura and C. Adachi, *Nature*, 2012, **492**, 234–238.
45 A. Rajca, *Chem. Rev.*, 1994, **94**, 871–893.
46 N. M. Gallagher, A. Olankitwanit and A. Rajca, *J. Org. Chem.*, 2015, **80**, 1291–1298.
47 A. Rajca, A. Olankitwanit and S. Rajca, *J. Am. Chem. Soc.*, 2011, **133**, 4750–4753.
48 Y. Joo, V. Agarkar, S. H. Sung, B. M. Savoie and B. W. Boudouris, *Science*, 2018, **359**, 1391–1395.
49 A. Rajca, J. Wongsriratanakul and S. Rajca, *Science*, 2001, **294**, 1503–1505.
50 G. Gryn'ova, M. L. Coote and C. Corminboeuf, *Wiley Interdiscip. Rev.: Comput. Mol. Sci.*, 2015, **5**, 440–459.
51 J. Autschbach, *J. Chem. Educ.*, 2012, **89**, 1032–1040.
52 M. P. Melrose and E. R. Scerri, *J. Chem. Educ.*, 1996, **73**, 498.
53 L. Abella, J. Crassous, L. Favereau and J. Autschbach, *Chem. Mater.*, 2021, **33**, 3678–3691.
54 R. Murata, Z. Wang, Y. Miyazawa, I. Antol, S. Yamago and M. Abe, *Org. Lett.*, 2021, **23**, 4955–4959.
55 R. Murata, Z. Wang and M. Abe, *Aust. J. Chem.*, 2021, **74**, 827.
56 Y. Wang, H. Zhang, M. Pink, A. Olankitwanit, S. Rajca and A. Rajca, *J. Am. Chem. Soc.*, 2016, **138**, 7298–7304.
57 A. Kumar and M. D. Sevilla, *J. Phys. Chem. B*, 2018, **122**, 98–105.
58 A. Izuoka, M. Hiraishi, T. Abe, T. Sugawara, K. Sato and T. Takui, *J. Am. Chem. Soc.*, 2000, **122**, 3234–3235.
59 H. Sakurai, A. Izuoka and T. Sugawara, *J. Am. Chem. Soc.*, 2000, **122**, 9723–9734.
60 J. Nakazaki, I. Chung, M. M. Matsushita, T. Sugawara, R. Watanabe, A. Izuoka and Y. Kawada, *J. Mater. Chem.*, 2003, **13**, 1011–1022.
61 H. Komatsu, R. Mogi, M. M. Matsushita, T. Miyagi, Y. Kawada and T. Sugawara, *Polyhedron*, 2009, **28**, 1996–2000.
62 M. Souto, C. Rovira, I. Ratera and J. Veciana, *CrystEngComm*, 2017, **19**, 197–206.
63 E. J. Baerends, *Mol. Phys.*, 2020, **118**, e1612955.

64 R. Baer, E. Livshits and U. Salzner, *Annu. Rev. Phys. Chem.*, 2010, **61**, 85–109.
65 J. Autschbach and M. Srebro, *Acc. Chem. Res.*, 2014, **47**, 2592–2602.
66 R. G. Parr and Y. Weitao, *Density-Functional Theory of Atoms and Molecules*, Oxford University Press, New York, 1995.
67 B. L. Westcott, N. E. Gruhn, L. J. Michelsen and D. L. Lichtenberger, *J. Am. Chem. Soc.*, 2000, **122**, 8083–8084.
68 M. J. Bialek and L. Latos-Grazynski, *Inorg. Chem.*, 2016, **55**, 1758–1769.
69 A. Idec, M. Pawlicki and L. Latos-Grazynski, *Inorg. Chem.*, 2017, **56**, 10337–10352.
70 K. R. Glaesemann and M. W. Schmidt, *J. Phys. Chem. A*, 2010, **114**, 8772–8777.
71 O. V. Gritsenko and E. J. Baerends, *J. Chem. Phys.*, 2004, **120**, 8364–8372.
72 T. Sugawara, H. Komatsu and K. Suzuki, *Chem. Soc. Rev.*, 2011, **40**, 3105–3118.
73 H. Guo, Q. Peng, X. K. Chen, Q. Gu, S. Dong, E. W. Evans, A. J. Gillett, X. Ai, M. Zhang, D. Credgington, V. Coropceanu, R. H. Friend, J. L. Bredas and F. Li, *Nat. Mater.*, 2019, **18**, 977–984.
74 S. Kasemthaveechok, L. Abella, M. Jean, M. Cordier, T. Roisnel, N. Vanthuyne, T. Guizouarn, O. Cador, J. Autschbach, J. Crassous and L. Favereau, *J. Am. Chem. Soc.*, 2020, **142**, 20409–20418.
75 W. Wang, L. Wang, S. Chen, W. Yang, Z. Zhang and X. Wang, *Sci. China: Chem.*, 2018, **61**, 300.
76 N. Gallagher, H. Zhang, T. Junghoefer, E. Giangrisostomi, R. Ovsyannikov, M. Pink, S. Rajca, M. B. Casu and A. Rajca, *J. Am. Chem. Soc.*, 2019, **141**, 4764–4774.
77 T. Kanetomo, K. Ichihashi, M. Enomoto and T. Ishida, *Org. Lett.*, 2019, **21**, 3909–3912.
78 B. Tang, J. Zhao, J.-F. Xu and X. Zhang, *Chem. Sci.*, 2020, **11**, 1192–1204.
79 C. Shu, H. Zhang, A. Olankitwanit, S. Rajca and A. Rajca, *J. Am. Chem. Soc.*, 2019, **141**, 17287–17294.
80 R. Zhao, K. Fu, Y. Fang, J. Zhou and L. Shi, *Angew. Chem., Int. Ed.*, 2020, **59**, 20682–20690.
81 E. Levernier, K. Jaouadi, H.-R. Zhang, V. Corcé, A. Bernard, G. Gontard, C. Troufflard, L. Grimaud, E. Derat, C. Ollivier and L. Fensterbank, *Chem.–Eur. J.*, 2021, **27**, 8782–8790.
82 T. Sugimoto, S. Yamaga, M. Nakai, K. Ohmori, M. Tsujii, H. Nakatsuji, H. Fujita and J. Yamauchi, *Chem. Lett.*, 1993, **22**, 1361–1364.
83 K. Ishiguro, M. Ozaki, N. Sekine and Y. Sawaki, *J. Am. Chem. Soc.*, 1997, **119**, 3625–3626.
84 S. Matsumiya, A. Izuoka, T. Sugawara, T. Taruishi and Y. Kawada, *Bull. Chem. Soc. Jpn.*, 1993, **66**, 513–522.
85 R. Kumai, M. M. Matsushita, A. Izuoka and T. Sugawara, *J. Am. Chem. Soc.*, 1994, **116**, 4523–4524.
86 R. Kumai, H. Sakurai, A. Izuoka and T. Sugawara, *Mol. Cryst. Liq. Cryst.*, 1996, **279**, 133–138.
87 H. Sakurai, R. Kumai, A. Izuoka and T. Sugawara, *Chem. Lett.*, 1996, **25**, 879–880.
88 J. Nakazaki, M. M. Matsushita, A. Izuoka and T. Sugawara, *Tetrahedron Lett.*, 1999, **40**, 5027–5030.
89 W. T. Borden and E. R. Davidson, *J. Am. Chem. Soc.*, 1977, **99**, 4587–4594.
90 D. Velasco, S. Castellanos, M. López, F. López-Calahorra, E. Brillas and L. Juliá, *J. Org. Chem.*, 2007, **72**, 7523–7532.
91 Z. Cui, A. Abdurahman, X. Ai and F. Li, *CCS Chem.*, 2020, **2**, 1129–1145.
92 J. Nakazaki, I. Chung, M. M. Matsushita, T. Sugawara, R. Watanabe, A. Izuoka and Y. Kawada, *J. Mater. Chem.*, 2003, **13**, 1011–1022.
93 J. Nakazaki, I. Chung, R. Watanabe, T. Ishitsuka, Y. Kawada, M. M. Matsushita and T. Sugawara, *Internet Electron. J. Mol. Des.*, 2003, **2**, 112–127.
94 I. Matsumoto, I. Ciofini, P. P. Laine and Y. Teki, *Chemistry*, 2009, **15**, 11210–11220.
95 Y. Orimoto, F. L. Gu, J. Korchowiec, A. Imamura and Y. Aoki, *Theor. Chem. Acc.*, 2009, **125**, 493–501.
96 A. Ito, R. Kurata, Y. Noma, Y. Hirao and K. Tanaka, *J. Org. Chem.*, 2016, **81**, 11416–11420.
97 J. Nakazaki, Y. Ishikawa, A. Izuoka, T. Sugawara and Y. Kawada, *Chem. Phys. Lett.*, 2000, **319**, 385–390.
98 A. Izuoka, M. Hiraishi, T. Abe, T. Sugawara, K. Sato and T. Takui, *J. Am. Chem. Soc.*, 2000, **122**, 3234–3235.
99 M. h. Chahma, K. Macnamara, A. van der Est, A. Alberola, V. Polo and M. Pilkington, *New J. Chem.*, 2007, **31**, 1973.
100 M. M. Matsushita, H. Kawakami, Y. Kawada and T. Sugawara, *Chem. Lett.*, 2007, **36**, 110–111.
101 M. M. Matsushita, H. Kawakami, T. Sugawara and M. Ogata, *Phys. Rev. B: Condens. Matter Mater. Phys.*, 2008, **77**, 195208.
102 H. Komatsu, M. M. Matsushita, S. Yamamura, Y. Sugawara, K. Suzuki and T. Sugawara, *J. Am. Chem. Soc.*, 2010, **132**, 4528–4529.
103 J. Guasch, L. Grisanti, V. Lloveras, J. Vidal-Gancedo, M. Souto, D. C. Morales, M. Vilaseca, C. Sissa, A. Painelli, I. Ratera, C. Rovira and J. Veciana, *Angew. Chem., Int. Ed.*, 2012, **51**, 11024–11028.
104 H. Douib, M. Puget, Y. Suffren, F. Pointillart, K. Bernot, B. Le Guennic, O. Cador, A. Gouasmia and L. Ouahab, *Dyes Pigm.*, 2017, **145**, 285–293.
105 T. Sugawara and M. M. Matsushita, *J. Mater. Chem.*, 2009, **19**, 1738–1753.
106 T. Kusamoto, S. Kume and H. Nishihara, *J. Am. Chem. Soc.*, 2008, **130**, 13844–13845.
107 T. Kusamoto, S. Kume and H. Nishihara, *Angew. Chem., Int. Ed.*, 2010, **49**, 529–531.
108 H.-B. Zhao, Y.-Q. Qiu, C.-G. Liu, S.-L. Sun, Y. Liu and R.-S. Wang, *J. Organomet. Chem.*, 2010, **695**, 2251–2257.
109 X. Zhang, S. Suzuki, M. Kozaki and K. Okada, *J. Am. Chem. Soc.*, 2012, **134**, 17866–17868.
110 G. Gryn'ova, D. L. Marshall, S. J. Blanksby and M. L. Coote, *Nat. Chem.*, 2013, **5**, 474.
111 G. Gryn'ova and M. L. Coote, *J. Am. Chem. Soc.*, 2013, **135**, 15392–15403.
112 P. Franchi, E. Mezzina and M. Lucarini, *J. Am. Chem. Soc.*, 2014, **136**, 1250–1252.

113 A. Tanushi, S. Kimura, T. Kusamoto, M. Tominaga, Y. Kitagawa, M. Nakano and H. Nishihara, *J. Phys. Chem. C*, 2019, **123**, 4417–4423.
114 Z. Wang, R. Murata and M. Abe, *ACS Omega*, 2021, **6**, 22773–22779.
115 Z. Wang, R. Akisaka, S. Yabumoto, T. Nakagawa, S. Hatano and M. Abe, *Chem. Sci.*, 2021, **12**, 613–625.
116 K. Awaga, T. Sugano and M. Kinoshita, *Chem. Phys. Lett.*, 1987, **141**, 540–544.
117 K. Awaga, T. Sugano and M. Kinoshita, *Chem. Phys. Lett.*, 1986, **128**, 587–590.
118 K. Awaga, T. Sugano and M. Kinoshita, *J. Chem. Phys.*, 1986, **85**, 2211–2218.
119 K. Awaga, T. Sugano and M. Kinoshita, *Solid State Commun.*, 1986, **57**, 453–456.
120 K. Karon and M. Lapkowski, *J. Solid State Chem.*, 2015, **19**, 2601–2610.
121 L. E. MacKenzie and P. Stachelek, *Nat. Chem.*, 2021, **13**, 521–522.
122 L. Frederic, A. Desmarchelier, L. Favereau and G. Pieters, *Adv. Funct. Mater.*, 2021, **31**, 2010281.
123 J. R. Brandt, F. Salerno and M. J. Fuchter, *Nat. Rev. Chem.*, 2017, **1**, 0045.
124 S. H. Yang, R. Naaman, Y. Paltiel and S. S. P. Parkin, *Nat. Rev. Phys.*, 2021, **3**, 328–343.
125 X. B. Shang, L. Wan, L. Wang, F. Gao and H. Y. Li, *J. Mater. Chem. C*, 2022, **10**, 2400–2410.
126 A. Ueda, H. Wasa, S. Suzuki, K. Okada, K. Sato, T. Takui and Y. Morita, *Angew. Chem., Int. Ed.*, 2012, **51**, 6691–6695.
127 B. D. Gliemann, A. G. Petrovic, E. M. Zolnhofer, P. O. Dral, F. Hampel, G. Breitenbruch, P. Schulze, V. Raghavan, K. Meyer, P. L. Polavarapu, N. Berova and M. Kivala, *Chem.–Asian J.*, 2017, **12**, 31–35.
128 M. V. Ivanov, K. Thakur, A. Bhatnagar and R. Rathore, *Chem. Commun.*, 2017, **53**, 2748–2751.
129 Y. C. Hsieh, C. F. Wu, Y. T. Chen, C. T. Fang, C. S. Wang, C. H. Li, L. Y. Chen, M. J. Cheng, C. C. Chueh, P. T. Chou and Y. T. Wu, *J. Am. Chem. Soc.*, 2018, **140**, 14357–14366.
130 Y. Inoue, D. Sakamaki, Y. Tsutsui, M. Gon, Y. Chujo and S. Seki, *J. Am. Chem. Soc.*, 2018, **140**, 7152–7158.
131 M. Narita, T. Teraoka, T. Murafuji, Y. Shiota, K. Yoshizawa, S. Mori, H. Uno, S. Kanegawa, O. Sato, K. Goto and F. Tani, *Bull. Chem. Soc. Jpn.*, 2019, **92**, 1867–1873.
132 R. Prince, Š. Tomáš, R. Michel, H. Daniel, N. Markus, B. Martin and J. Michal, *Angew. Chem., Int. Ed.*, 2016, **55**, 1183–1186.
133 P. Ravat, T. Solomek, D. Haussinger, O. Blacque and M. Juricek, *J. Am. Chem. Soc.*, 2018, **140**, 10839–10847.
134 C. Shen, G. Loas, M. Srebro-Hooper, N. Vanthuyne, L. Toupet, O. Cador, F. Paul, J. T. L. Navarrete, F. J. Ramirez, B. Nieto-Ortega, J. Casado, J. Autschbach, M. Vallet and J. Crassous, *Angew. Chem., Int. Ed.*, 2016, **55**, 8062–8066.
135 P. Mayorga-Burrezo, V. G. Jimenez, D. Blasi, T. Parella, I. Ratera, A. G. Campana and J. Veciana, *Chem.–Eur. J.*, 2020, **26**, 3776–3781.
136 P. M. Burrezo, V. G. Jimenez, D. Blasi, I. Ratera, A. G. Campana and J. Veciana, *Angew. Chem., Int. Ed.*, 2019, **58**, 16282–16288.
137 S. Shil, D. Bhattacharya, A. Misra and D. J. Klein, *Phys. Chem. Chem. Phys.*, 2015, **17**, 23378–23383.
138 J. S. J. Tan and R. S. Paton, *Chem. Sci.*, 2019, **10**, 2285–2289.
139 S. Zhang, X. Liu, C. Li, L. Li, J. Song, J. Shi, M. Morton, S. Rajca, A. Rajca and H. Wang, *J. Am. Chem. Soc.*, 2016, **138**, 10002–10010.
140 A. Rajca, C. Shu, H. Zhang, S. Zhang, H. Wang and S. Rajca, *Photochem. Photobiol.*, 2021, **97**, 1376–1390.
141 T. Tsuchiya, Y. Katsuoka, K. Yoza, H. Sato and Y. Mazaki, *ChemPlusChem*, 2019, **84**, 1659–1667.
142 J. K. Zak, M. Miyasaka, S. Rajca, M. Lapkowski and A. Rajca, *J. Am. Chem. Soc.*, 2010, **132**, 3246–3247.
143 J. R. Brandt, X. Wang, Y. Yang, A. J. Campbell and M. J. Fuchter, *J. Am. Chem. Soc.*, 2016, **138**, 9743–9746.
144 P. Josse, L. Favereau, C. Shen, S. Dabos-Seignon, P. Blanchard, C. Cabanetos and J. Crassous, *Chem.–Eur. J.*, 2017, **23**, 6277–6281.
145 Y. Yang, R. C. da Costa, M. J. Fuchter and A. J. Campbell, *Nat. Photonics*, 2013, **7**, 634.
146 K. Ishii, S. Hattori and Y. Kitagawa, *Photochem. Photobiol. Sci.*, 2020, **19**, 8–19.
147 M. Atzori, G. Rikken and C. Train, *Chem.–Eur. J.*, 2020, **26**, 9784–9791.
148 R. Naaman, Y. Paltiel and D. H. Waldeck, *Nat. Rev. Chem.*, 2019, **3**, 250–260.
149 A. K. Mondal, M. D. Preuss, M. L. Śleczkowski, T. K. Das, G. Vantomme, E. W. Meijer and R. Naaman, *J. Am. Chem. Soc.*, 2021, **143**, 7189–7195.
150 D. H. Waldeck, R. Naaman and Y. Paltiel, *APL Mater.*, 2021, **9**, 040902.